

FMNL2 Drives Actin-Based Protrusion and Migration Downstream of Cdc42

Jennifer Block,¹ Dennis Breitsprecher,^{2,8} Sonja Kühn,³ Moritz Winterhoff,² Frieda Kage,¹ Robert Geffers,⁴ Patrick Duwe,⁵ Jennifer L. Rohn,⁶ Buzz Baum,⁶ Cord Brakebusch,⁷ Matthias Geyer,³ Theresia E.B. Stradal,^{4,5} Jan Faix,² and Klemens Rottner^{1,4,*}

¹Institute of Genetics, University of Bonn, Karlrobert-Kreiten-Strasse 13, 53115 Bonn, Germany

²Institute for Biophysical Chemistry, Hannover Medical School, Carl-Neuberg-Strasse 1, 30623 Hannover, Germany

³Max Planck Institute of Molecular Physiology, Otto-Hahn-Strasse 11, 44227 Dortmund, Germany

⁴Helmholtz Centre for Infection Research, Inhoffenstrasse 7, 38124 Braunschweig, Germany

⁵Institute for Molecular Cell Biology, University of Münster, Schlossplatz 5, 48149 Münster, Germany

⁶MRC Laboratory for Molecular Cell Biology, University College London, London WC1E 6BT, UK

⁷BRIC, University of Copenhagen, Ole Maaløes Vej 5, 2200 Copenhagen, Denmark

Summary

Cell migration entails protrusion of lamellipodia, densely packed networks of actin filaments at the cell front. Filaments are generated by nucleation, likely mediated by Arp2/3 complex and its activator Scar/WAVE [1]. It is unclear whether formins contribute to lamellipodial actin filament nucleation or serve as elongators of filaments nucleated by Arp2/3 complex [2]. Here we show that the Diaphanous-related formin FMNL2, also known as FRL3 or FHOD2 [3], accumulates at lamellipodia and filopodia tips. FMNL2 is cotranslationally modified by myristoylation and regulated by interaction with the Rho-guanosine triphosphatase Cdc42. Abolition of myristoylation or Cdc42 binding interferes with proper FMNL2 activation, constituting an essential prerequisite for subcellular targeting. In vitro, C-terminal FMNL2 drives elongation rather than nucleation of actin filaments in the presence of profilin. In addition, filament ends generated by Arp2/3-mediated branching are captured and efficiently elongated by the formin. Consistent with these biochemical properties, RNAi-mediated silencing of FMNL2 expression decreases the rate of lamellipodia protrusion and, accordingly, the efficiency of cell migration. Our data establish that the FMNL subfamily member FMNL2 is a novel elongation factor of actin filaments that constitutes the first Cdc42 effector promoting cell migration and actin polymerization at the tips of lamellipodia.

Results and Discussion

Diaphanous-related formins are regulated by autoinhibition, typically released by interaction with guanosine triphosphate

(GTP)-bound, active versions of specific Rho family guanosine triphosphatases (GTPases) [3, 4]. They can generate bundles composed of linear actin filaments, like those found in microvilli or filopodia [5]. Among 15 human formins, Drf3 (murine version, mDia2) is established best to induce filopodia [6–8], but its role in lamellipodia formation is ambiguous because its RNAi-mediated knockdown both inhibited [8] and promoted [9] lamellipodia. Although expression of active Drf3 variants drives explosive filopodia formation [6, 8], redundancy with related formins is likely [10], because we observed no RNAi phenotype in HeLa cells (J.B. and K.R., unpublished data).

To find additional formins operating in lamellipodia and filopodia protrusion, we first explored formin messenger RNA (mRNA) expression in a panel of human and murine cell lines using microarrays. Whereas mDia2/Drf3 messages were mostly absent in motile murine fibroblasts or B16-F1 cells [6], we found significant Diaphanous-related formin FMNL2/FRL3 mRNA (Figure 1A) and protein (Figure 1B) in all cell lines. Interestingly, high FMNL2 expression correlated with increased invasiveness of colorectal cancer cells [11, 12], suggesting a role in cell migration. In murine cells, the antibody originally raised against FMNL2 also cross-reacted with a smaller protein (Figure 1B), confirmed by RNAi to correspond to the closely related FMNL3/FRL2 (see Figure S3G available online) [3, 13]. Accordingly, we only detected FMNL3/FRL2 mRNA in murine cell lines (Figure 1A), whereas the mostly hematopoietic FMNL1/FRL1 appeared below threshold in all lines, in agreement with western blotting (F.K. and K.R., unpublished data). FMNL2 harbors the canonical domains of a Diaphanous-related formin—the autoregulatory DID and DAD domains, and the FH1-FH2 module proposed to mediate actin assembly [4] (Figure 1C). FMNL2 has two splice isoforms with slight C-terminal sequence variation [14]: the A (short) and B (long) variants (Figure 1C). As before [15], all experiments shown here were done with the B variant. Immunolabelings revealed prominent staining of endogenous FMNL2/FMNL3 in lamellipodia (Figure 1D; Figure S1A), suggesting involvement in actin-based protrusion. Lamellipodial accumulation of FMNL2 was confirmed by video microscopy of the same cell type expressing an enhanced green fluorescent protein (EGFP)-tagged variant, rendered active through DAD domain truncation (Figure 1E; Movie S1). Like active Drf3-ΔDAD [6] or different, active FMNL3 variants [13], activated FMNL2 also accumulated at filopodial tips (Figure 1E), but unlike Drf3-ΔDAD [6], it did not suppress lamellipodia, indicating that FMNL2 (and perhaps FMNL3) might be involved in both filopodia and lamellipodia formation (Figure 1E). Accumulation in the lamellipodium was abolished during retraction (Figure 1E, asterisk), as expected for a potential protrusion regulator, but unusually, FMNL2 could also associate with retracting or tail edges (Movie S1). Moreover, FMNL2 dislocalized much more slowly than vasodilator-stimulated phosphoprotein (VASP) during lamellipodial retraction (Figures S1B and S1C), suggesting tight association with and regulation of lamellipodial actin filaments. We confirmed specific enrichment of FMNL2ΔDAD in lamellipodia with an inert volume marker (Figure S1D), Arp2/3 complex staining (Figure S1E),

⁸Present address: Rosenstiel Basic Medical Science Research Center, Brandeis University, 415 South Street, Waltham, MA 02454, USA

*Correspondence: krottner@uni-bonn.de

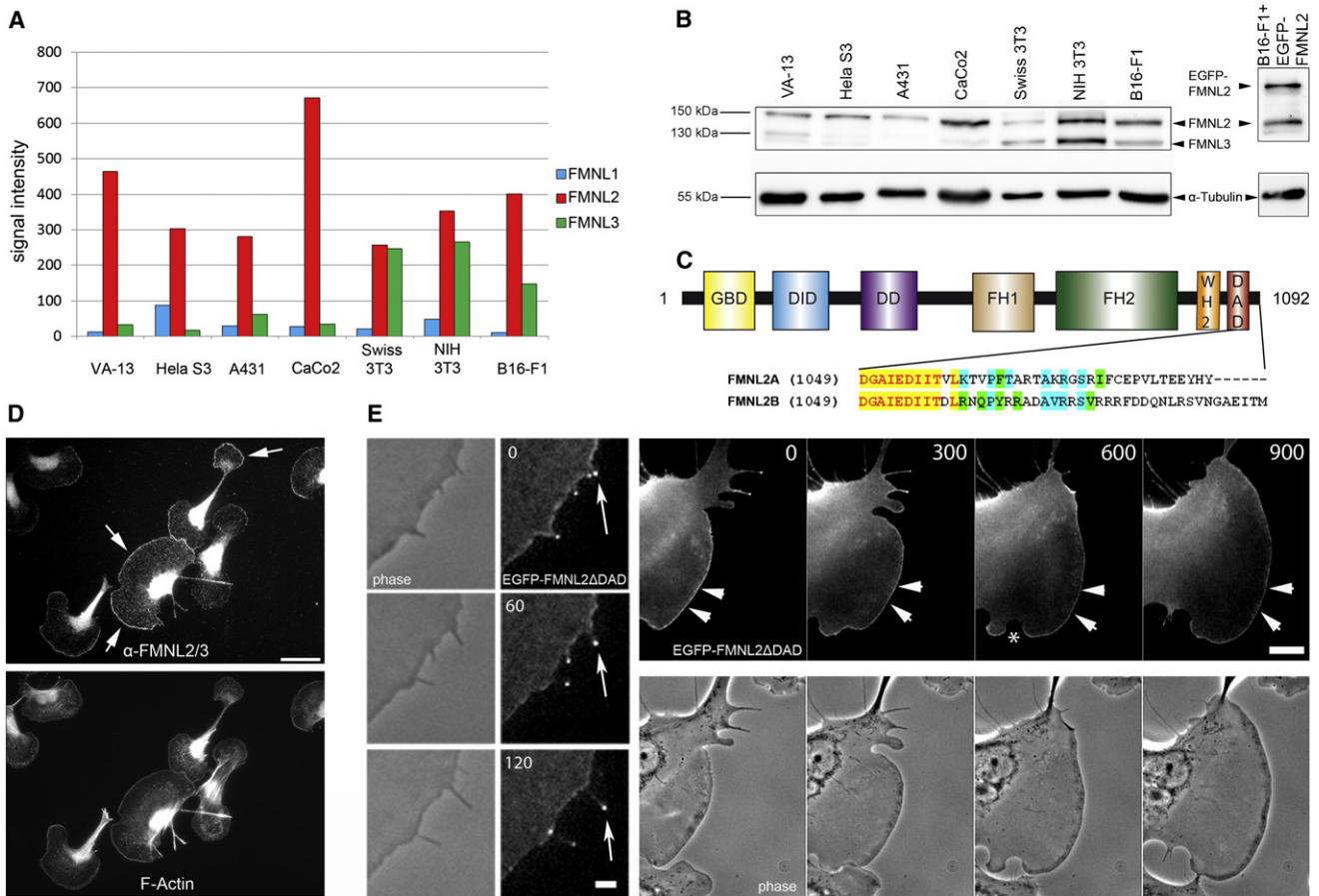


Figure 1. FMNL2 Is Widely Expressed and Accumulates at the Tips of Lamellipodia and Filopodia

(A) Microarray analyses indicating high levels of FMNL2 gene transcription in various murine and human cell lines. (B) Confirmation of FMNL2 expression by western blotting in cell lines as in (A). α -tubulin was used as loading control; FMNL2 migrates at an apparent molecular weight of 150 kDa plus \sim 30 kDa for the EGFP-tagged variant. The additional band most prominent in murine cell lines corresponded to FMNL3 (Figure S3G), as indicated. (C) Domain structure and splice variants of FMNL2 are illustrated. DID, Diaphanous inhibitory domain; DD, dimerization domain; FH1/2, formin homology 1/2; WH2, WASP homology 2; DAD, Diaphanous autoregulatory domain. FMNL2 is spliced into at least two isoforms, designated FMNL2A (Uniprot identifier Q96PY5-1) and FMNL2B (Uniprot identifier Q96PY5-3), which differ at their C-terminal ends as depicted. (D) Immunolabeling showing that endogenous FMNL2/FMNL3 are concentrated in F-actin-rich lamellipodia (white arrows, zoom-in: Figure S1A) of B16-F1 melanoma cells. Scale bar represents 30 μ m. (E) EGFP-tagged, constitutively active FMNL2 (Δ DAD) targets to the tips of protruding filopodia (white arrows) and lamellipodia (white arrowheads) but is displaced in the course of retraction (asterisk; see also Figures S1B and S1C). Time is in s; scale bars represent 2 μ m (left panel) and 10 μ m (right panel).

and by colocalization with VASP or the WAVE complex subunit *Abi-1* (Figure S1F). Despite its proposed function as bundling protein [15], we observed no colocalization with fascin and bundled actin in microspikes (Figure S1F).

Next, we determined potential interactions of FMNL2 with specific Rho-GTPases. Pull-down experiments using GST- or MBP-tagged GTPases and EGFP-tagged FMNL2 variants harboring the GTPase binding domain (GBD) (Figure 1C) showed nucleotide-dependent interactions with Cdc42 and Rac1, but not RhoA, RhoD, Rif, or RhoG (Figure S2A; positive controls in Figure S2B). GST-Cdc42 or -Rac1 variants could also directly pull down purified FMNL2 residues 1–489 (FMNL2_{NCC}), proving direct interactions and indicating Cdc42 being much more effective (Figure S2D). Using isothermal titration calorimetry (ITC), the purified N terminus of FMNL2 (FMNL2_N) exclusively interacted with Cdc42 associated with the nonhydrolyzable GTP analog GppNhp (Figure 2A), but not with GDP-loaded Cdc42 (Figure 2B) nor with active

Rac1 (Figure 2C). We conclude that FMNL2 is a specific downstream effector of Cdc42 but likely not of related small GTPases such as Rac1 or RhoA.

In cells, ectopically expressed EGFP-tagged FMNL2 was entirely cytosolic (Figure 2D), presumably due to autoinhibition [6], but potentially targeted to the cell periphery upon coexpression of constitutively active Cdc42 (Figure 2D). Consistent with the ITC data, coexpression of constitutively active Rac1 did not cause peripheral targeting, although the latter induced prominent lamellipodia (Figure 2D), nor did coexpression of EGFP-FMNL2 with constitutively active RhoA (Figure S2G) or RhoC (Figure S2H), despite strong stress fiber induction. Again, FMNL2_N failed to interact with active RhoA in ITC assays (Figure S2E). Together, these data establish FMNL2 as the first Cdc42 effector capable of targeting to the tips of lamellipodia.

Besides interaction with Rho-GTPases, formins might be regulated by protein modifications. For instance, FMNL1 was

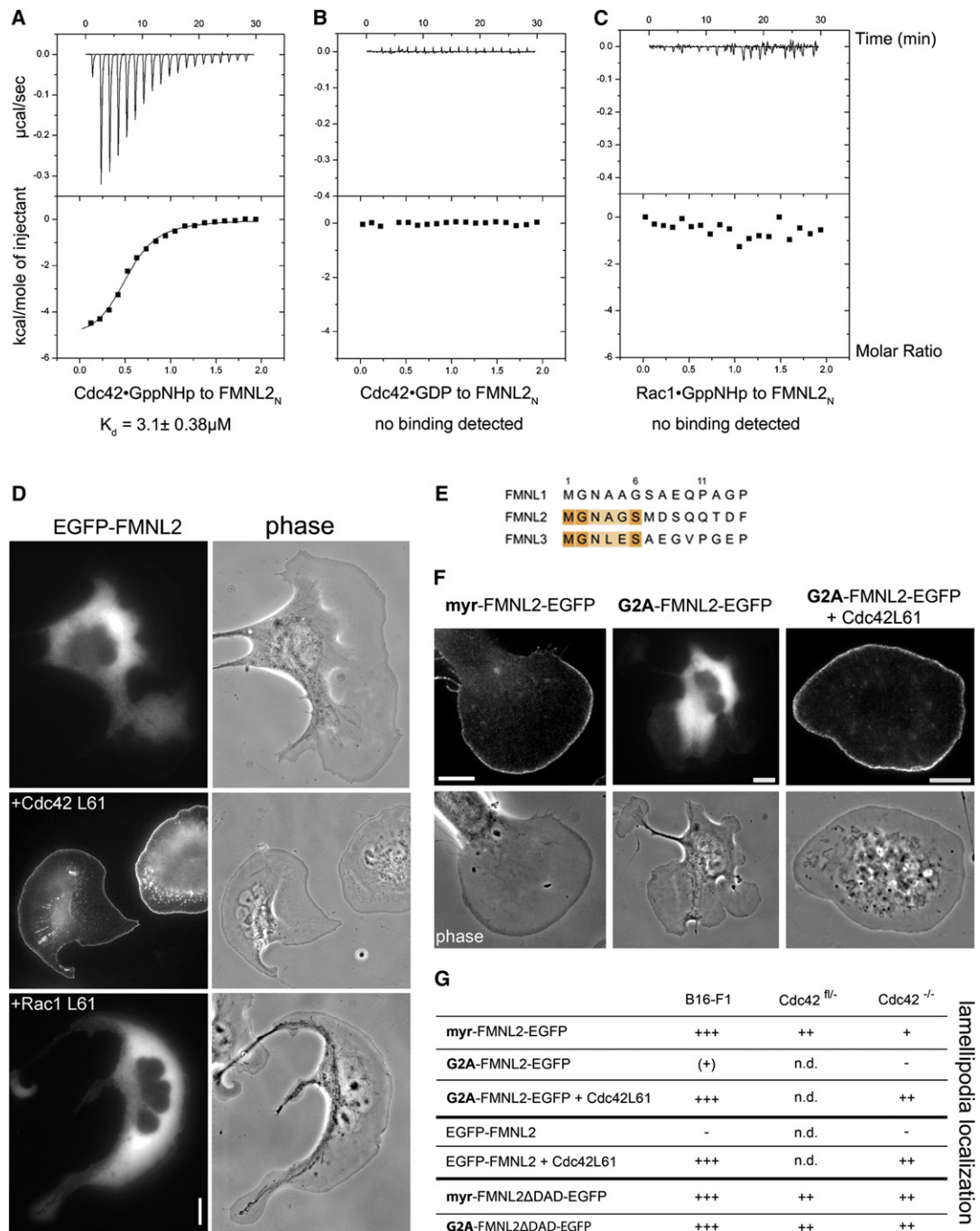


Figure 2. FMNL2 Is Regulated by Cdc42 and Myristoylation

(A–C) ITC measurements of the interactions between triphosphate-loaded Rho-GTPases and purified FMNL2 N terminus (FMNL2_N, aa 2–379). (A) Binding of Cdc42·GppNHp to FMNL2_N revealed a dissociation constant (K_D) of $3.13 \pm 0.38 \mu\text{M}$. ΔH and ΔS corresponded to $-5.33 \pm 0.16 \text{ kcal/mol}$ and 2.19 kcal/mol , respectively, with a molar ratio of 0.51. No binding was detected with either diphosphate-loaded Cdc42 (B) or Rac1·GppNHp (C).

(D) Subcellular targeting of FMNL2 is affected by constitutively active Cdc42, but not Rac1. EGFP-FMNL2 expressed in B16-F1 cells is entirely cytosolic (top) but targeted to the cell periphery upon coexpression of active Cdc42 (middle). Constitutively active Rac1 (bottom) lacked this effect, consistent with ITC measurements (C) and despite significant lamellipodia stimulation. Scale bar represents $10 \mu\text{m}$.

(E) FMNL2 and FMNL3 (but not FMNL1) harbor the canonical myristoylation consensus sequence MGXXXS at their N termini.

(F) FMNL2B capable of myristoylation due to C-terminal tagging with EGFP (myr-FMNL2-EGFP) targets to protruding lamellipodia in B16-F1 cells (left), but an analogous construct harboring a point mutation prohibiting myristoylation (G2A-FMNL2-EGFP) does not (middle). Targeting of G2A-FMNL2-EGFP is restored by coexpression with constitutively active Cdc42 (right). Scale bars represent $10 \mu\text{m}$.

(G) Myristoylation and Cdc42 both mediate activation of FMNL2, but not its subcellular targeting. Summary of subcellular localization of constructs as depicted in B16-F1 cells or fibroblasts lacking Cdc42 (Cdc42^{-/-}) and their parental controls (Cdc42^{fl/-}). For images see Figures S3A and S3B. Specific accumulation in the lamellipodium was categorized as follows: +++, very strong localization; ++, clear, specific enrichment; +, weak enrichment; (+), weak localization in some but not all cells examined; (-), no enrichment; n.d., not determined. Note that nonmyristoylatable, active FMNL2 (G2A-FMNL2 Δ DAD-EGFP) localizes to lamellipodia even in Cdc42^{-/-} cells.

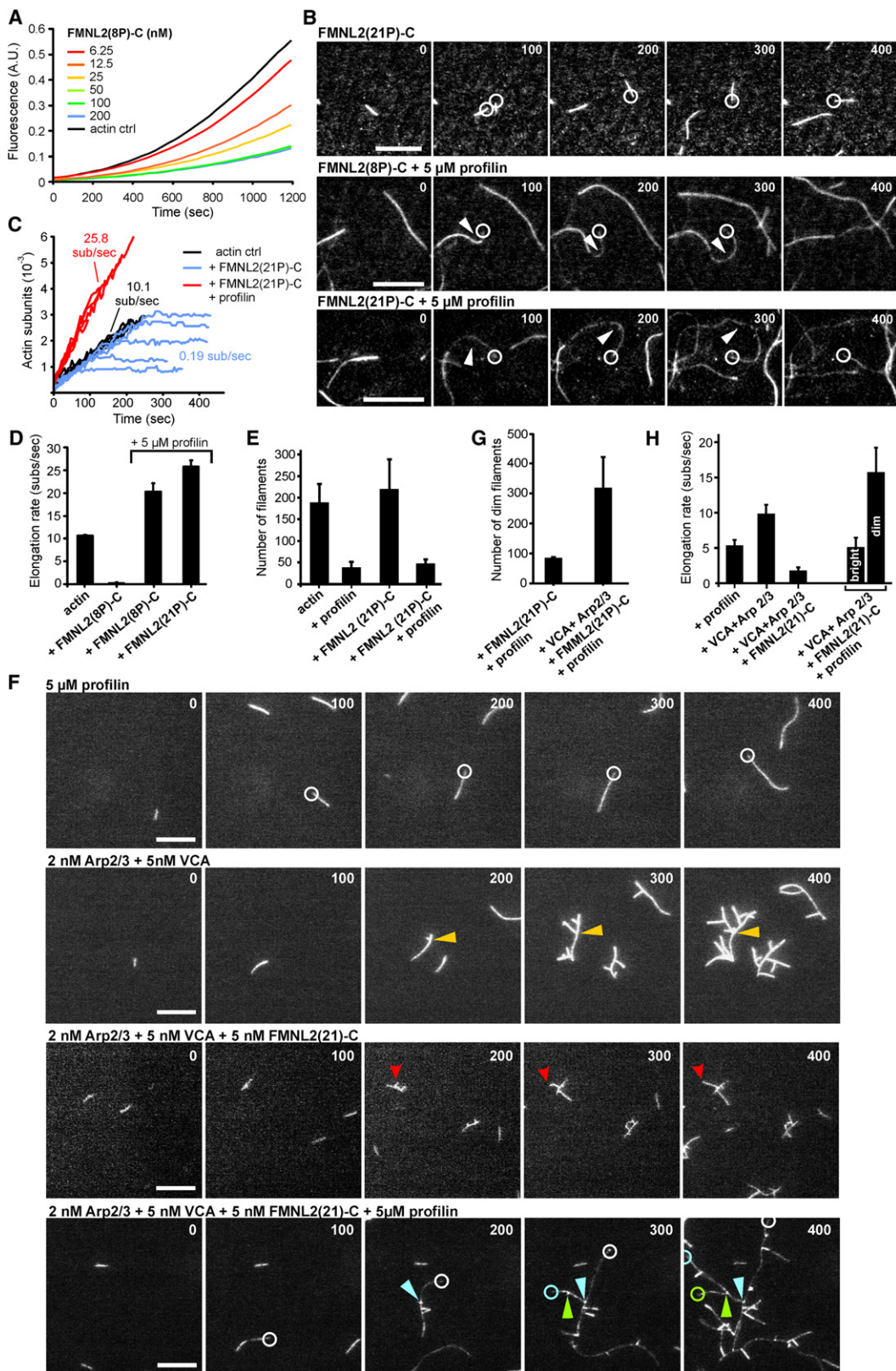


Figure 3. FMNL2 Requires Profilin to Elongate Actin Filaments Derived from Spontaneous or Arp2/3 Complex-Mediated Nucleation
(A) FMNL2 inhibits actin polymerization in the absence of profilin. A total of 3 μ M G-actin (10% pyrene labeled) was polymerized in 1 \times KMEI buffer in the presence of FMNL2(8P)-C at concentrations as indicated.
(B) FMNL2 processively assembles actin filaments. Spontaneous assembly of 1.3 μ M actin (23% Alexa 488 labeled) in the presence of 20 nM FMNL2(8P)-C (top) or 5 nM FMNL2(8P)-C and 5 μ M profilin (middle) or 10 nM FMNL2(21P)-C and 5 μ M profilin (bottom) monitored by TIRFM. Circles mark barbed ends

previously suggested to be myristoylated [16], and indeed, both FMNL2 and FMNL3 harbor the canonical consensus sequence for N-terminal myristoylation [17] (Figure 2E). Consistently, mass spectrometry proved that ectopically expressed FMNL2_N can be myristoylated in *E. coli* (Figures S2I–S2K). N-terminal protein tagging blocks N-terminal myristoylation [17], so to test whether myristoylation contributes to subcellular targeting and/or activation of FMNL2, we fused EGFP C-terminally to the full-length formin. Strikingly, unlike the N-terminally tagged protein (Figure 2D), this variant (myr-FMNL2-EGFP) localized to lamellipodia tips in B16-F1 cells even in the absence of Rho-GTPase coexpression (Figure 2F; Movie S2), similar to the active, EGFP-ΔDAD variant (Figure 1E). Importantly, this effect was largely abolished by a G→A mutation at position 2 (Figure 2F), proving its dependence on myristoylation, but was reverted by ectopic coexpression of constitutively active Cdc42 (Figures 2F and 2G). Systematic analysis of subcellular targeting of FMNL2 variants in B16-F1 cells compared to fibroblasts heterozygous or homozygous null for the Cdc42 gene [18] established that both myristoylation and active Cdc42 contribute to FMNL2 activation. Subcellular targeting, however, also occurred in the absence of both signals, given that the formin lacked the DAD domain required for autoinhibition (Figure 2G; for representative images see Figures S3A and S3B). Unlike previous suggestions [16, 19], our data demonstrate that FMNL2 lipidation and Rho-GTPase interaction are dispensable for accumulation in lamellipodia and filopodia but, instead, control release from autoinhibition at or close to the plasma membrane. Finally, myristoylation does also not significantly affect FMNL2 interaction with Cdc42, assayed by either pull-down or ITC (Figures S2C and S2F). The recruitment factor to the tips of lamellipodia and filopodia remains unknown.

To explore how FMNL2 influences actin dynamics, we expressed and purified fragments from the C-terminal half of FMNL2, comprising the FH1 and FH2 domains essential for actin assembly in most formins [4], as well as the WH2 and DAD domains (Figure 1C). FH1 and FH2 domains work together in actin assembly by interactions with the actin-monomer binding proteins profilin and actin, respectively [4], but for FMNL3, the WH2 domain has also been implicated in actin binding [20]. In FMNL2, the wild-type FH1 sequence harbors long stretches of consecutive proline residues thought to recruit profilin-actin complexes [4]. To aid bacterial expression, we engineered synthetic variants of C-terminal FMNL2 with modified numbers of consecutive FH1 domain prolines, FMNL2(8P)-C and FMNL2(21P)-C (for purity see Figure S3C). FMNL2(8P)-C inhibited actin polymerization

in pyrene-actin assays in a concentration-dependent manner (Figure 3A; Figure S3D), likely mediated by formin interaction with the fast-growing barbed ends of actin filaments (K_{app} of ~18 nM; see Figure S3D), leading to interference with their elongation. Consistently, FMNL2(8P)-C also protected filaments from depolymerization, although not as efficiently as heterodimeric capping protein (Figure S3E). FMNL2(21)-C also inhibited pyrene-actin assembly (data not shown).

To test formin action at the barbed end more directly, we performed total internal reflection fluorescence microscopy (TIRFM) to visualize and quantify individual actin filament barbed ends growing in the presence or absence of the formin and profilin. Without either factor, barbed ends grew at a rate of ~10 subunits/s (Figure 3D; data not shown). In contrast, addition of FMNL2(8P)-C (data not shown) or FMNL2(21P)-C alone abrogated barbed-end growth (Figures 3B–3D; Movie S3). However, profilin addition induced assembly of dim, fast-growing filaments, as reported for other formins that prefer to incorporate nonlabeled actin under these conditions [21] (Figures 3B–3D). Also, frequent filament buckling was observed (Figure 3B; Movie S3), likely caused by formin molecules passively attaching to the coverslip surface, and indicative of processive barbed-end elongation. As opposed to other formins like mDia2 (Figure S3F), both FMNL2 fragments did not significantly change the number of filaments observed (data not shown; Figure 3E), regardless of the presence of profilin. Addition of the latter to actin alone strongly reduced filament numbers, as expected, but similar values were obtained upon further addition of FMNL2(21P)-C (Figure 3E). These results differ somewhat from a report that the FMNL3 C terminus could accelerate actin assembly even in the absence of profilin [20], but whether this was due to nucleation or severing remained uncertain [13]. Our data suggest that FMNL2 is at best a very weak nucleator but can processively elongate actin filaments in the presence of profilin. Within the lamellipodium, filaments, presumably nucleated by Arp2/3 complex [22, 23], could be captured and elongated by FMNL2. To test whether FMNL2 could elongate filaments generated by Arp2/3-mediated branching, we assayed FMNL2 with or without profilin in the presence of Arp2/3 complex and its activator Scar1-VCA (see also Movie S4). Activated Arp2/3 complex generated growing filament networks harboring multiple branches, which was reduced by FMNL2(21)-C alone (Figure 3F), presumably because barbed ends were efficiently capped. However, profilin addition enabled accelerated growth of dim filament ends (as in the absence of Arp2/3 complex), frequently originating in bright filament branch

captured by FMNL2 molecules passively absorbed to the coverslip; arrows indicate dim, buckling filaments elongated by FMNL2. Time is in seconds. Scale bars represent 10 μm. See Movie S3.

(C) Examples of individual, spontaneously growing, or FMNL2(21P)-C-assembled filaments increasing in length over time in the presence or absence of profilin.

(D) Quantification of actin filament elongation rates as determined by TIRFM.

(E) FMNL2 does not significantly enhance nucleation in the absence or presence of profilin. Filament numbers counted for actin alone or upon addition of profilin (5 μM) or FMNL2(21P)-C (10 nM), or both, as indicated.

(F) FMNL2 elongates actin filaments nucleated by Arp2/3 complex. Spontaneous assembly of 1.3 μM actin (23% ATTO 488 labeled) in the presence of the proteins indicated. Arrowheads mark branch points generated by Arp2/3 complex, except for red ones that mark branch and/or filament end capped by FMNL2 in the absence of profilin. White circles mark barbed ends of spontaneously growing filaments, and green, blue, or white circles at the bottom mark dim filaments elongated by FMNL2. Scale bars represent 5 μm. See Movie S4.

(G) Quantification of filaments elongated by FMNL2(21P)-C and profilin in the presence or absence of activated Arp2/3 complex at concentrations as in (F).

(H) Quantification of actin filament elongation from experiments as shown in (G).

Error bars in (D), (E), (G), and (H) represent mean ± SD from at least three independent measurements.

See Figure S3.

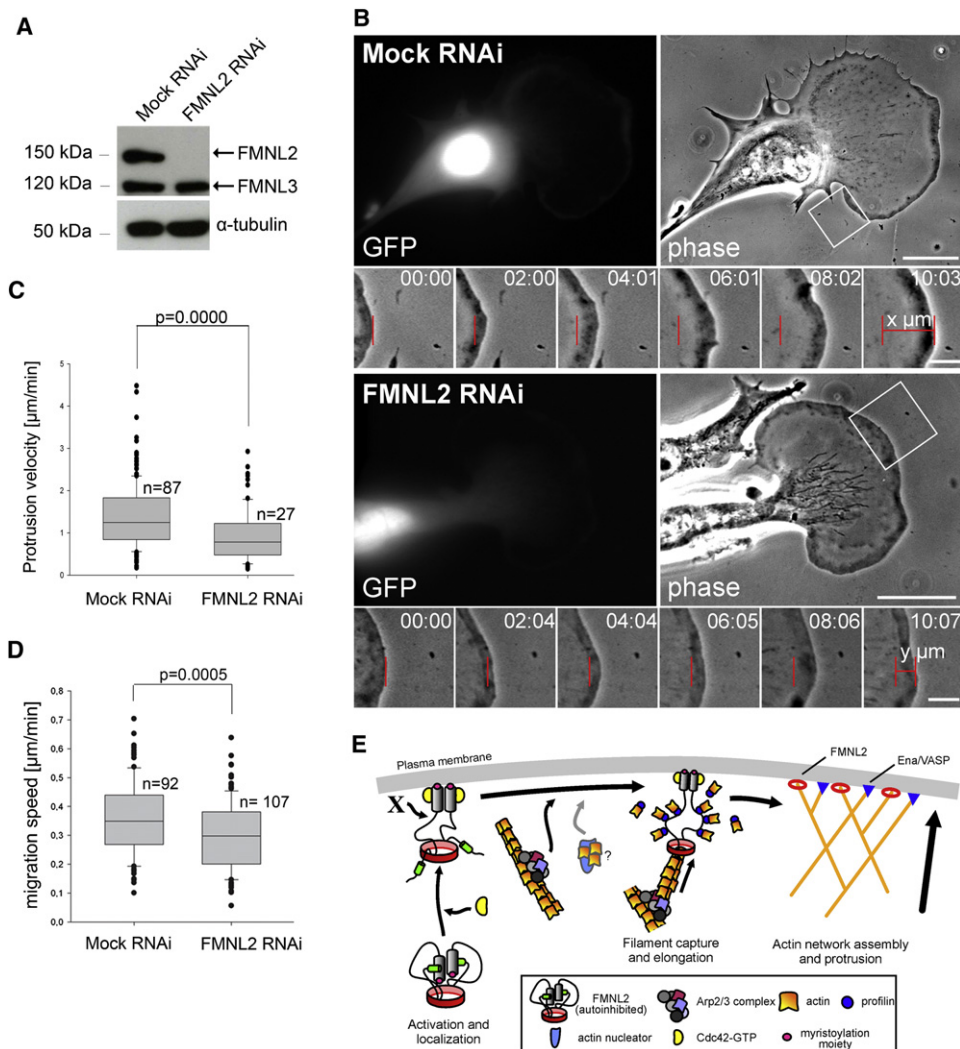


Figure 4. FMNL2 Regulates Rates of Lamellipodia Protrusion and Cell Migration

(A) Western blot using anti-FMNL2 antibody and extracts from B16-F1 cells transfected with mock construct or a vector mediating knockdown of FMNL2 (FMNL2 RNAi). α -tubulin was used as a loading control.

(B) Analysis of protrusion rates of lamellipodia formed in mock or FMNL2 knockdown cells, with transfected cells identified by GFP expression. Insets show representative regions from images recorded by phase-contrast time-lapse microscopy and subjected to protrusion rate analyses as indicated. Time is in minutes and seconds; scale bars in overview panels represent 20 μm and in insets 5 μm .

(C) Box and whisker plots showing results from quantification of lamellipodia protrusion velocities in mock (arithmetic mean, 1.26 $\mu\text{m}/\text{min}$; SD, 0.62 $\mu\text{m}/\text{min}$) and FMNL2 knockdown cells (arithmetic mean, 0.96 $\mu\text{m}/\text{min}$; SD, 0.62 $\mu\text{m}/\text{min}$). The line within the box indicates median, and the box boundaries contain 50% (25%–75%) and the whiskers 80% (10%–90%) of all measurements, whereas outlying points are shown as dots. Difference in protrusion velocity was confirmed to be statistically significant by Mann-Whitney rank sum test.

(D) Migration efficiency of B16-F1 control (arithmetic mean, 0.36 $\mu\text{m}/\text{min}$; SD, 0.13 $\mu\text{m}/\text{min}$) versus FMNL2 knockdown cells (arithmetic mean, 0.298 $\mu\text{m}/\text{min}$; SD, 0.12 $\mu\text{m}/\text{min}$). Data were displayed and confirmed to be statistically significant as in (C). Data in (C) and (D) are derived from at least three independent experiments.

(E) Model for FMNL2 function in lamellipodium protrusion is illustrated. Actin filaments are generated by nucleation through Arp2/3 complex or perhaps alternative mechanisms (actin nucleator). Engagement of FMNL2 is preceded by release from autoinhibition possibly mediated by a myristoyl switch (not shown) and by interaction with active Cdc42. FMNL2 dimers then capture preformed actin filament barbed ends and promote their elongation in a profilin/actin-dependent manner. Elongation by FMNL2 is proposed to accelerate lamellipodium protrusion in coordination with other factors, e.g., the Ena/VASP family member VASP. Cdc42 contributes to activation but not recruitment of FMNL2 to the lamellipodium tip, which is mediated by an unknown factor (X) remaining to be established.

See Figure S3 and Movie S5.

points (Figure 3F; Movie S4). Quantification of the number of dim filaments in the presence or absence of activated Arp2/3 complex confirmed that most formin-captured, dim filaments were nucleated by Arp2/3 complex (Figure 3G). Elongation rates of individual filaments in all these conditions were also quantified (Figure 3H). Profilin decreased elongation

rates versus actin alone (Figure 3D) to about 5 subunits/s (Figure 3H) due to the reduced rate constant for association of profilin-actin with barbed ends [24]. Growth of filaments nucleated by Arp2/3 complex (Figure 3H) was identical to spontaneously nucleated ones (Figure 3D), as expected, whereas further addition of FMNL2(21)-C in these conditions

markedly suppressed their growth (Figure 3H). In contrast, the simultaneous presence of activated Arp2/3 complex, FMNL2(21)-C, and profilin generated two populations of growing filaments: bright ones elongating at about 5 subunits/s—presumably not captured by the formin—and dim ones growing at 15 subunits/s (Figure 3H) apparently accelerated by the formin in the presence of profilin-actin. These data constitute the first demonstration of Arp2/3 complex and a formin collaborating in actin assembly through promoting filament branching and elongation, respectively, and suggest that FMNL2 might exert similar functions in protruding lamellipodia.

Although Cdc42 is essential for wound-healing migration in fibroblasts [18], it can drive cell shape changes and induce filopodia and lamellipodia formation, thus promoting migration in certain conditions [25]. It is currently unclear whether Cdc42 regulates lamellipodial protrusion only through Rac [26, 27], as deduced from experiments using dominant-negative GTPases [28], or also by direct interaction with downstream effectors regulating actin dynamics. A role for the Cdc42 effector N-WASP in lamellipodial Arp2/3 activation is unlikely due to its absence in the lamellipodium and the lack of a phenotype in null fibroblasts [29]. Signaling to actin dynamics through a formin is an attractive alternative. We thus asked whether interference with FMNL2 function abrogated or modified the formation and dynamics of lamellipodia. We silenced FMNL2 expression in motile B16-F1 melanoma cells using RNAi, which did not affect FMNL3 (Figure 4A; Figure S3G). Although lamellipodia did form, their protrusion velocities were markedly reduced (76.2%) compared to controls. Measurements of protrusion rates using phase-contrast optics were restricted to transfected, GFP-positive cells (Figure 4B; Movie S5). The protrusion velocities of lamellipodia formed by B16-F1 cells migrating on laminin can be correlated with accumulation of lamellipodial tip markers such as VASP [30] and, presumably, rate of actin polymerization [31]. We speculate that lack of FMNL2 at the lamellipodium tip reduces elongation rates of lamellipodial actin filaments and, thus, rate of forward translocation. Whether FMNL3 might serve functions similar or differential to FMNL2 is currently unknown. However, these and previous data suggest that Cdc42, e.g., through its effector FMNL2, tunes lamellipodial protrusion by regulating actin filament elongation rather than nucleation, a function likely reserved for the Rac/WAVE/Arp2/3 pathway [1, 22, 23]. Interestingly, *Drosophila* S2R+ cells silenced for the sole fly FMNL ortholog CG32138 stood out in a recent genome-wide screen for factors regulating cell shape [32], displaying lamellipodia with abnormal morphology (Figure S3H). These data suggest that core functions of FMNL-like factors developed early and remained conserved throughout evolution. Inefficient lamellipodium protrusion as seen upon FMNL2 knock-down should impair B16-F1 migration, and indeed, this was observed (Figure 4D).

In conclusion, our data uncover a novel signaling pathway linking the Rho family GTPase Cdc42 to activation of the FMNL subfamily member FMNL2 in migrating mesenchymal cells. Cdc42 thus promotes lamellipodium protrusion and migration by at least two separate mechanisms: (i) by indirect signaling to Rac activation [26, 27], and (ii) by directly activating FMNL formins modulating actin polymerization rate at the lamellipodium tip. Future work should establish the precise relevance of Arp2/3 complex versus different formins or actin filament polymerases of the Ena/VASP family [33, 34] in lamellipodium protrusion.

Supplemental Information

Supplemental Information includes three figures, Supplemental Experimental Procedures, and five movies and can be found with this article online at doi:10.1016/j.cub.2012.03.064.

Acknowledgments

This work was supported in part by the Deutsche Forschungsgemeinschaft (DFG) grants RO2414/3-1 (to K.R.), FA330/4-2 and FA330/6-1 (to J.F.), and GE-976/7 (to M.G.). We would like to thank P. Aspenström, A. Hall, L. Machesky, G. Scita, and R. Tsien for reagents and B. Denker, P. Hagen-dorff, and G. Landsberg for technical assistance.

Received: December 6, 2011

Revised: March 2, 2012

Accepted: March 29, 2012

Published online: May 17, 2012

References

1. Campellone, K.G., and Welch, M.D. (2010). A nucleator arms race: cellular control of actin assembly. *Nat. Rev. Mol. Cell Biol.* 11, 237–251.
2. Ridley, A.J. (2011). Life at the leading edge. *Cell* 145, 1012–1022.
3. Schönichen, A., and Geyer, M. (2010). Fifteen formins for an actin filament: a molecular view on the regulation of human formins. *Biochim. Biophys. Acta* 1803, 152–163.
4. Chesarone, M.A., DuPage, A.G., and Goode, B.L. (2010). Unleashing formins to remodel the actin and microtubule cytoskeletons. *Nat. Rev. Mol. Cell Biol.* 11, 62–74.
5. Faix, J., and Rottner, K. (2006). The making of filopodia. *Curr. Opin. Cell Biol.* 18, 18–25.
6. Block, J., Stradal, T.E., Hänisch, J., Geffers, R., Köstler, S.A., Urban, E., Small, J.V., Rottner, K., and Faix, J. (2008). Filopodia formation induced by active mDia2/Drf3. *J. Microsc.* 231, 506–517.
7. Pellegrin, S., and Mellor, H. (2005). The Rho family GTPase Rif induces filopodia through mDia2. *Curr. Biol.* 15, 129–133.
8. Yang, C., Czech, L., Gerboth, S., Kojima, S., Scita, G., and Svitkina, T. (2007). Novel roles of formin mDia2 in lamellipodia and filopodia formation in motile cells. *PLoS Biol.* 5, e317.
9. Beli, P., Mascheroni, D., Xu, D., and Innocenti, M. (2008). WAVE and Arp2/3 jointly inhibit filopodium formation by entering into a complex with mDia2. *Nat. Cell Biol.* 10, 849–857.
10. Ramalingam, N., Zhao, H., Breitsprecher, D., Lappalainen, P., Faix, J., and Schleicher, M. (2010). Phospholipids regulate localization and activity of mDia1 formin. *Eur. J. Cell Biol.* 89, 723–732.
11. Zhu, X.L., Liang, L., and Ding, Y.Q. (2008). Overexpression of FMNL2 is closely related to metastasis of colorectal cancer. *Int. J. Colorectal Dis.* 23, 1041–1047.
12. Zhu, X.L., Zeng, Y.F., Guan, J., Li, Y.F., Deng, Y.J., Bian, X.W., Ding, Y.Q., and Liang, L. (2011). FMNL2 is a positive regulator of cell motility and metastasis in colorectal carcinoma. *J. Pathol.* 224, 377–388.
13. Harris, E.S., Gauvin, T.J., Heimsath, E.G., and Higgs, H.N. (2010). Assembly of filopodia by the formin FRL2 (FMNL3). *Cytoskeleton (Hoboken)* 67, 755–772.
14. Katoh, M., and Katoh, M. (2003). Identification and characterization of human FMNL1, FMNL2 and FMNL3 genes in silico. *Int. J. Oncol.* 22, 1161–1168.
15. Vaillant, D.C., Copeland, S.J., Davis, C., Thurston, S.F., Abdennur, N., and Copeland, J.W. (2008). Interaction of the N- and C-terminal autoregulatory domains of FRL2 does not inhibit FRL2 activity. *J. Biol. Chem.* 283, 33750–33762.
16. Han, Y., Eppinger, E., Schuster, I.G., Weigand, L.U., Liang, X., Kremmer, E., Peschel, C., and Krackhardt, A.M. (2009). Formin-like 1 (FMNL1) is regulated by N-terminal myristoylation and induces polarized membrane blebbing. *J. Biol. Chem.* 284, 33409–33417.
17. Resh, M.D. (2006). Trafficking and signaling by fatty-acylated and prenylated proteins. *Nat. Chem. Biol.* 2, 584–590.
18. Czuchra, A., Wu, X., Meyer, H., van Hengel, J., Schroeder, T., Geffers, R., Rottner, K., and Brakebusch, C. (2005). Cdc42 is not essential for filopodium formation, directed migration, cell polarization, and mitosis in fibroblastoid cells. *Mol. Biol. Cell* 16, 4473–4484.

19. Seth, A., Otomo, C., and Rosen, M.K. (2006). Autoinhibition regulates cellular localization and actin assembly activity of the diaphanous-related formins FRLalpha and mDia1. *J. Cell Biol.* **174**, 701–713.
20. Heimsath, E.G., Jr., and Higgs, H.N. (2012). The C-terminus of the formin FMNL3 accelerates actin polymerization and contains a WH2-like sequence that binds both monomers and filament barbed ends. *J. Biol. Chem.* **287**, 3087–3098.
21. Kovar, D.R., Harris, E.S., Mahaffy, R., Higgs, H.N., and Pollard, T.D. (2006). Control of the assembly of ATP- and ADP-actin by formins and profilin. *Cell* **124**, 423–435.
22. Nicholson-Dykstra, S.M., and Higgs, H.N. (2008). Arp2 depletion inhibits sheet-like protrusions but not linear protrusions of fibroblasts and lymphocytes. *Cell Motil. Cytoskeleton* **65**, 904–922.
23. Steffen, A., Faix, J., Resch, G.P., Linkner, J., Wehland, J., Small, J.V., Rottner, K., and Stradal, T.E. (2006). Filopodia formation in the absence of functional WAVE- and Arp2/3-complexes. *Mol. Biol. Cell* **17**, 2581–2591.
24. Romero, S., Le Clainche, C., Didry, D., Egile, C., Pantaloni, D., and Carlier, M.F. (2004). Formin is a processive motor that requires profilin to accelerate actin assembly and associated ATP hydrolysis. *Cell* **119**, 419–429.
25. Monypenny, J., Zicha, D., Higashida, C., Oceguera-Yanez, F., Narumiya, S., and Watanabe, N. (2009). Cdc42 and Rac family GTPases regulate mode and speed but not direction of primary fibroblast migration during platelet-derived growth factor-dependent chemotaxis. *Mol. Cell. Biol.* **29**, 2730–2747.
26. Baird, D., Feng, Q., and Cerione, R.A. (2005). The Cool-2/alpha-Pix protein mediates a Cdc42-Rac signaling cascade. *Curr. Biol.* **15**, 1–10.
27. Nishimura, T., Yamaguchi, T., Kato, K., Yoshizawa, M., Nabeshima, Y., Ohno, S., Hoshino, M., and Kaibuchi, K. (2005). PAR-6-PAR-3 mediates Cdc42-induced Rac activation through the Rac GEFs STEF/Tiam1. *Nat. Cell Biol.* **7**, 270–277.
28. Nobes, C.D., and Hall, A. (1995). Rho, rac, and cdc42 GTPases regulate the assembly of multimolecular focal complexes associated with actin stress fibers, lamellipodia, and filopodia. *Cell* **81**, 53–62.
29. Lommel, S., Benesch, S., Rottner, K., Franz, T., Wehland, J., and Kühn, R. (2001). Actin pedestal formation by enteropathogenic *Escherichia coli* and intracellular motility of *Shigella flexneri* are abolished in N-WASP-defective cells. *EMBO Rep.* **2**, 850–857.
30. Rottner, K., Behrendt, B., Small, J.V., and Wehland, J. (1999). VASP dynamics during lamellipodia protrusion. *Nat. Cell Biol.* **1**, 321–322.
31. Lai, F.P., Szczodrak, M., Block, J., Faix, J., Breitsprecher, D., Mannherz, H.G., Stradal, T.E., Dunn, G.A., Small, J.V., and Rottner, K. (2008). Arp2/3 complex interactions and actin network turnover in lamellipodia. *EMBO J.* **27**, 982–992.
32. Rohn, J.L., Sims, D., Liu, T., Fedorova, M., Schöck, F., Dopie, J., Vartiainen, M.K., Kiger, A.A., Perrimon, N., and Baum, B. (2011). Comparative RNAi screening identifies a conserved core metazoan actinome by phenotype. *J. Cell Biol.* **194**, 789–805.
33. Breitsprecher, D., Kieseewetter, A.K., Linkner, J., Vinzenz, M., Stradal, T.E., Small, J.V., Curth, U., Dickinson, R.B., and Faix, J. (2011). Molecular mechanism of Ena/VASP-mediated actin-filament elongation. *EMBO J.* **30**, 456–467.
34. Hansen, S.D., and Mullins, R.D. (2010). VASP is a processive actin polymerase that requires monomeric actin for barbed end association. *J. Cell Biol.* **191**, 571–584.